

Electrostatic Switching in Vertically Oriented Nanotubes for Nonvolatile Memory Applications

Anupama B. Kaul,¹ Paul Khan,^{1,2} Andrew T. Jennings,³ Julia R. Greer,³ Krikor G. Megerian,¹
and Paul von Allmen¹

¹Jet Propulsion Laboratory, California Institute of Technology, Pasadena, CA 91109

²Keck School of Medicine, University of Southern California, Los Angeles, CA 90089

³Division of Applied Science and Engineering, California Institute of Technology, Pasadena, CA 91125

ABSTRACT

We have demonstrated electrostatic switching in vertically oriented nanotubes or nanofibers, where a nanoprobe was used as the actuating electrode inside an SEM. When the nanoprobe was manipulated to be in close proximity to a single tube, switching voltages between 10 V – 40 V were observed, depending on the geometrical parameters. The turn-on transitions appeared to be much sharper than the turn-off transitions which were limited by the tube-to-probe contact resistances. In many cases, stiction forces at these dimensions were dominant, since the tube appeared stuck to the probe even after the voltage returned to 0 V, suggesting that such structures are promising for nonvolatile memory applications. The stiction effects, to some extent, can be adjusted by engineering the switch geometry appropriately. Nanoscale mechanical measurements were also conducted on the tubes using a custom-built nanoindenter inside an SEM, from which preliminary material parameters, such as the elastic modulus, were extracted. The mechanical measurements also revealed that the tubes appear to be well adhered to the substrate. The material parameters gathered from the mechanical measurements were then used in developing an electrostatic model of the switch using a commercially available finite-element simulator. The calculated pull-in voltages appeared to be in agreement to the experimentally obtained switching voltages to first order.

INTRODUCTION

Performance limitations of Si integrated circuits as a result of continued miniaturization has created an ever-increasing need for exploring new materials and architectures beyond solid-state transistors. Nano-electro-mechanical (NEM) switches may overcome these limitations, by reducing leakage currents and power dissipation during operation, while at the same time providing the added benefits of enhanced radiation tolerance, and high temperature resilience.

Carbon nanotube (CNT) based NEMS have already been demonstrated in applications ranging from nanotweezers,¹ memory devices,² supersensitive sensors³ and tunable oscillators.⁴ To date, switching in both SWNTs² and MWNTs^{5,6,7} has been reported for deposited tubes that are parallel to the substrate. Here, we demonstrate switching results for vertically-oriented tubes, which are grown on-chip with Ni catalyst using plasma-enhanced chemical vapor deposition (PECVD). We will describe electrical characterizing results of these vertically oriented nanotubes, where a nanoprobe inside an SEM was used to actuate single tubes. Nanoscale mechanical characterization results will also be presented, where a custom nano-indenter was

used to observe deflection characteristics of individual tubes in an SEM under compressive loading. The mechanical properties of the tubes obtained empirically from the nanomechanical measurements were then used in the electrostatic model that was developed using a finite element simulator. The pull-in voltages obtained from simulation were then compared to the experimentally obtained switching voltages for a nominal geometry. Other models are also currently under development at JPL for similar structures, that are based on first principles calculations.^{8,9}

EXPERIMENTAL DETAILS

The tube growth was performed in a manner similar to that described elsewhere;¹⁰ in the electrical measurements described here, the tube growth was performed directly on metallic underlayers, the details of which will be presented elsewhere.¹¹ The sample which comprised of arrays of vertically oriented tubes, was then mounted on a 45° beveled edge on an Al holder, and placed inside an SEM. Consequently, all SEMs shown here have been taken at 45° with respect to the electron beam. A nanomanipulator probe stage (Kammrath and Weiss) was then mounted inside the SEM, where two tungsten probes from the stage were used to perform 2-terminal measurements on individual tubes with the aid of an HP4155C parameter analyzer.

DISCUSSION

Electrical Characterization

In Figure 1, shown is the current transport through an individual tube, when it is contacted with the tip of a nanoprobe as indicated by the SEM. The I-V characteristic depicts a tunnel barrier of some sort, which is not surprising since no special procedures were taken to remove the native oxide that may have potentially existed on the probe tip. The tubes were seen to cycle current repeatedly without showing signs of deterioration to compliances typically ~ 90 nA. However, as the current was increased steadily, the tubes started to deteriorate, and in many cases burned-up between 150 – 250 nA. Shown in the SEM of Fig. 2b is the same tube, that had been cycled several times to 100 nA (Fig. 1a inset), after which point a constriction appeared in the tube body that deteriorated its current response (Fig. 1b).

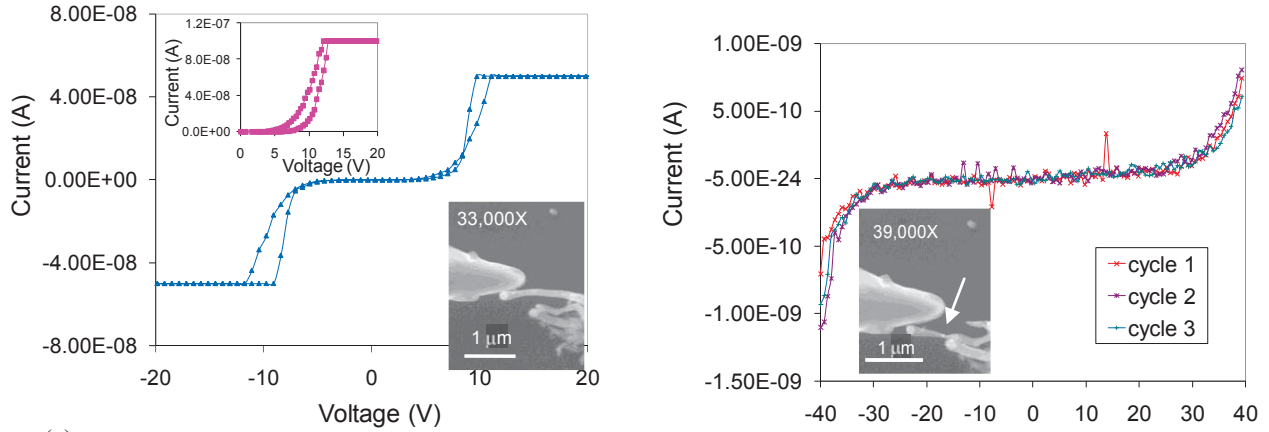


Figure 1. a) Electrical continuity measurements for a single tube in contact with the voltage probe as indicated by the SEM image. The inset shows that the compliance increased to 100 nA. (b) After several cycles at 100 nA, the tube appeared thinner, and a constriction appeared in the body (see arrow in SEM image) which deteriorated its current response.

Actuation measurements were then conducted where the tip of the nanoprobe was manipulated such that it was in close proximity to a single tube as shown in Fig. 2a. As the I-V characteristic indicates, the pull-in voltage for this tube was ~ 18 V. After reaching the 50 nA compliance, hysteresis was seen in the reverse cycle, where the turn-off occurred at a lower voltage ~ 16 V; the reverse cycle was also less pronounced. Fig. 2b captures another switching event for a tube, where the turn-on and turn-off occurred at ~ 14 V and 10 V, respectively. Figure 2b illustrates the abruptness of the turn-on transition compared to the turn-off transition.

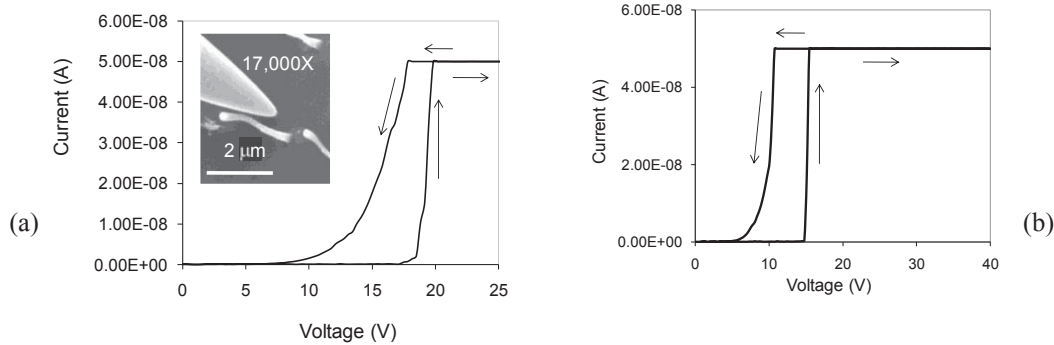


Figure 2. a) Actuation test of a nanoprobe in close proximity to the tube shown in the SEM. The turn-on is ~ 18 V. (b) Another case where the turn-on and turn-off occur at ~ 14 V and 10 V, respectively. The abruptness of the turn-on transition compared to the turn-off transition is exemplified here.

In Figure 3a, the SEM image shows a different tube just prior to actuation. This was a tube with length $L \sim 2.8 \mu\text{m}$, gap $G \sim 160$ nm, diameter $D \sim 60$ nm, and a probe-to-tube coupling length $C \sim 0.63 \mu\text{m}$. The image in Fig. 3b depicts that the tube is stuck to the probe after electrostatic actuation. The corresponding I-V shown in Fig. 3c indicates a switching voltage of ~ 26 V. The SEM in (b) indicates the tube remains in contact with the probe even when the voltage is removed. The stiction is captured in the I-V characteristic of Fig. 3c, which shows the less pronounced turn-off cycle that is attributed to the contact-resistance of the probe to the tube. The stiction forces indicate the van der Waals forces are strong at these dimensions, and suggest that these structures have promise in NEMS for nonvolatile memory applications.

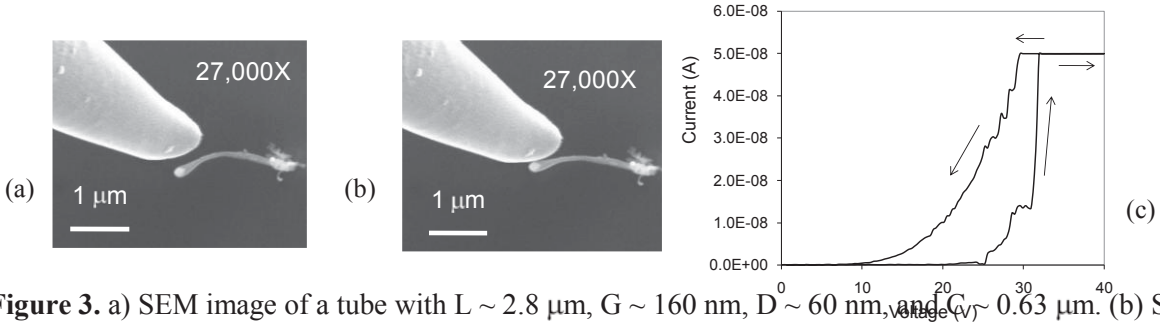


Figure 3. a) SEM image of a tube with $L \sim 2.8 \mu\text{m}$, $G \sim 160 \text{ nm}$, $D \sim 60 \text{ nm}$, and $G \sim 0.63 \mu\text{m}$. (b) SEM image of the same tube after actuation, depicting the tube is stuck to the probe. (c) The corresponding I-V characteristic for switching showing turn-on starting at $\sim 26 \text{ V}$. Tilt angle on all SEMs $\sim 45^\circ$.

The SEM image shown in Fig. 4a, shows the same tube but with a slightly larger gap between the probe and the tube. This larger gap suggests that the turn-on should occur at a larger voltage, and is validated experimentally by the corresponding I-V characteristic (Fig. 4c), which indicates a switching voltage of $\sim 32 \text{ V}$ (cycle 1). Although the SEM image in Fig. 4b shows the tube stuck to the probe after actuation, the contact area between the probe and the tip is extremely small; consequently, the tube detaches from the probe prior to the subsequent switching cycle. Figure 4c shows a second switching cycle for the same tube where the turn-on now is slightly higher $\sim 35 \text{ V}$, but the turn-off shows very little variation between the two cycles. When the gap is increased further as shown in the SEM of Fig. 4d, no switching is observed up to 40 V . The trends observed experimentally appear to confirm expectations, but more detailed comparisons will be made to the FEM simulations described shortly.

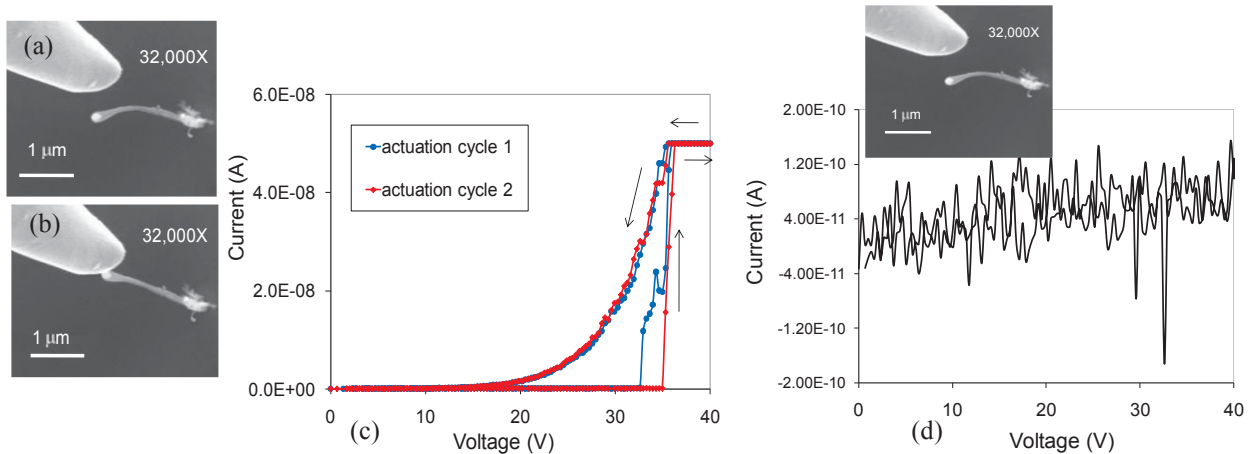


Figure 4. a) The gap for the same tube in Fig. 3a is now larger. (b) The tube is actuated, and is momentarily stuck to the probe when the SEM image is captured, but it detaches prior to the 2nd switching cycle. (c) Two switching cycles that show the turn-on varying slightly ($\sim 32 \text{ V}$ and 35 V) but there is little variation in the turn-off cycles. (d) No switching observed when the gap is increased further.

Nanomechanical Characterization

Nanoscale mechanical measurements were also conducted on the tubes using a custom-built nanoindenter inside an SEM, known as the SEMentor.¹² A Berkovich tip was loaded into the SEMentor, and a forest of tubes was indented (Fig. 5a). The CNTs were loaded until failure and the SEM image in Fig. 5b, taken after the test, suggests that the adhesion of the tubes to the Si

substrate is quite strong. The fracture point appears to be within the tube body since they do not necessarily detach from the substrate.

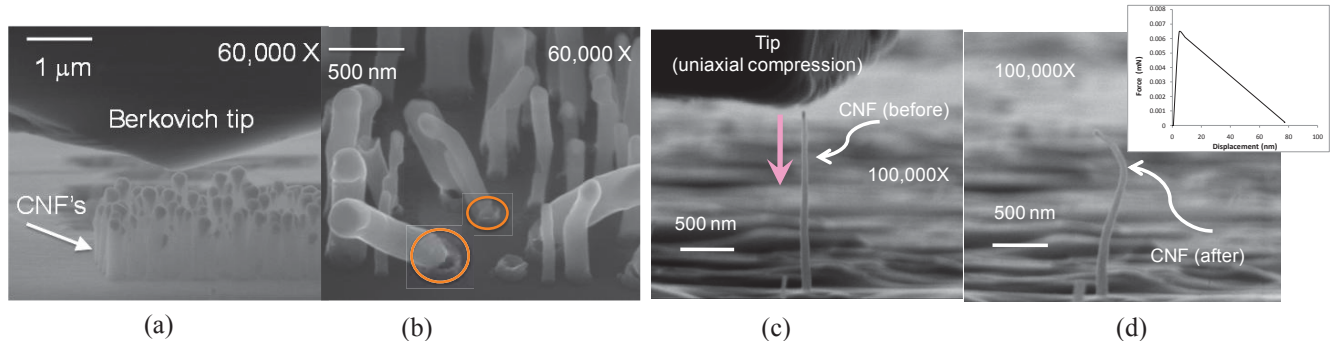
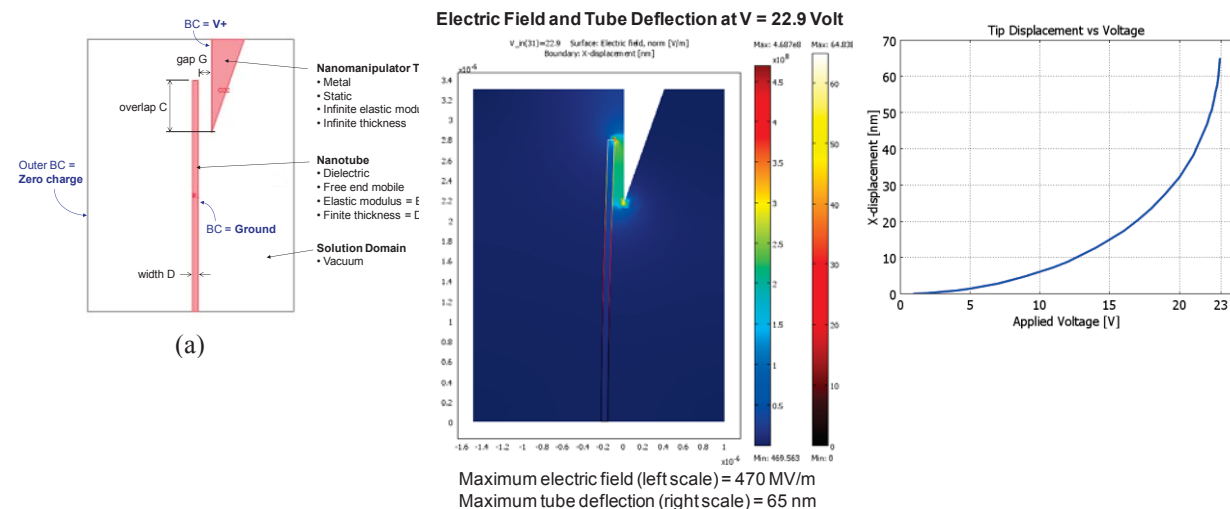


Figure 5. a) A Berkovich tip is used to mechanically bend a forest of tubes in a SEM (Ref. 2). (b) An SEM image of tubes taken after the mechanical bending tests, which indicates the tubes fracture at the base and do not necessarily detach from the substrate, suggesting the tube-to-substrate adhesion is strong. (c) A single tube is shown in close proximity to a tip which will load the tube in uniaxial compression. (d) The same tube is shown after it has buckled, with the corresponding force-deflection characteristic.

Furthermore, compression tests on the CNTs were initiated to determine materials parameters of the CNTs. The SEM image in Fig. 5c shows a single tube in close proximity to a tip just prior to the application of the load. Figure 5d illustrates the same tube after compression, where buckling was also observed. Although only a single tube is seen, it is not clear if other tubes were present and in contact with the tip as it moved down toward the substrate. Also, the large aspect ratio of the tubes, coupled with their tapered geometries were both sources of error when a modulus of ~ 600 GPa was computed from the force-deflection characteristic in the inset of Fig. 5d. The tube was assumed to have a length of $1.75\mu\text{m}$ and a diameter of 78nm , and was assumed to be structurally homogeneous. More measurements will be performed shortly to quantify these mechanical properties more accurately.

Electrostatic Modeling

We analyzed the interaction between the nanoprobe and the CNT using COMSOL Multiphysics, a commercially available finite element (FEM) analysis software package. Figure 6a illustrates the 2-D geometry used, along with the various boundary conditions.¹³ The pull-in voltage was calculated by numerically solving the coupled electrostatic interaction between the nanotube and the probe-tip. The nanotube was modeled as a dielectric rod with elastic modulus $E = 600$ GPa (as determined from the mechanical measurements), and the probe tip was modeled as a wedge subtracted from the solution volume. This effectively encompassed the properties of a metal tip with infinite stiffness, infinite thickness, and zero electric field components inside the tip volume.



(c)

(b)

Figure 6. (a) Geometry and electrical boundary conditions for coupled structural and electrostatic analysis of the CNT pull-in voltage. (b) Electric field distribution, and nanotube deflection for a nominal case (Fig. 3a) where $E = 600$ GPa (as deciphered from the nanomechanical measurements), $L = 2.8$ μm , $G = 160$ nm, $D = 60$ nm, $C = 0.63$ μm . (d) The nanotube tip displacement as a function of applied voltage for the nominal case defined above. The calculated pull-in voltage is noted to be 23 Volt, which appears to be in rough agreement with the measurements (turn-on ~ 26 V).

With this model, the spatial profile of the electric field was determined and is shown in Fig. 6b. As expected the field is concentrated at the tip where the deflection of the CNT is expected to be maximal. The pull-in voltage was obtained by plotting the tip deflection as a function of voltage, and noting the voltage at which the slope of the curve approaches infinity. As shown in Figure 6c, the calculated pull-in voltage for the nominal case was determined to be ~ 23 V. The switching voltage obtained experimentally for such parameters (Fig. 3a) was ~ 26 V, which appears to be in agreement, to first order, with the theoretically calculated value.

CONCLUSIONS

We have experimentally demonstrated electrostatic switching in vertically oriented PECVD grown nanotubes, where the switching voltages were in rough agreement with those computed numerically from simulations. In addition, nanomechanical measurements revealed that the tubes appeared to be well-adhered to the substrate, and preliminary materials parameters were also obtained. In conclusion, such structures show promise in NEMS for nonvolatile memory applications.

ACKNOWLEDGMENTS

We thank Dr. Choonsup Lee, Dr. Larry Epp and Dr. Richard Baron for useful discussions. We acknowledge assistance from Mr. Ron Ruiz with the SEM configuration. We also greatly acknowledge the use of facilities at the Kavli Nanoscience Institute at the California Institute of Technology, for enabling these *insitu* SEM measurements. This research was carried out at the Jet Propulsion Laboratory, California Institute of Technology, under a contract with the National Aeronautics and Space Administration and was funded through the internal Research and Technology Development (R&TD) program.

REFERENCES

-
- ¹ P. Kim and C. M. Lieber, *Science* **286**, 2148 (1999).
 - ² T. Rueckes, K. Kim, E. Joselevich, G. Y. Tseng, C. L. Cheung, and C. M. Lieber, *Science* **289**, 94 (2000).
 - ³ P. G. Collins, K. B. Bradley, M. Ishigamo, and A. Zettl, *Science* **287**, 120 (2000).
 - ⁴ V. Sazonova, Y. Yaish, H. Ustunel, D. Roundy, T. A. Arias, and P. L. McEuen, *Nature* **431**, 284 (2004).

-
- ⁵ S. W. Lee, D. S. Lee, R. E. Morjan, S. H. Jhang, M. Sveningsson, O. A. Nerushev, Y. W. Park, and E. E. B. Campbell, *Nano. Lett.* **4**, 2027 (2004).
- ⁶ S. N. Cha, J. E. Jang, Y. Choi, and G. A. J. Amaratunga, D. J. Kang, D. J. Hasko, J. E. Jung and J. M. Kim, *Appl. Phys. Lett.* **86**, 083105-1 (2005).
- ⁷ E. Dujardin, V. Derycke, M. F. Goffman, R. Lefevre, and J. P. Bourgoin, *Appl. Phys. Lett.* **87**, 193107-1 (2005).
- ⁸ P. von Allmen, T. Vo, K. G. Megerian, R.L Baron, and A. B. Kaul, to appear MRS Spring Meet. 2009.
- ⁹ Trin Vo, P. von Allmen, and A. B. Kaul, to appear MRS Spring Meeting Proc., 2009.
- ¹⁰ A. B. Kaul, K. Megerian, P. von Allmen, and R. L. Baron, *Nanotech.* **20**, 075303 (2009).
- ¹¹ A. B. Kaul, *et al.* manuscript in preparation, to be submitted.
- ¹² S. Brinkmann, J-Y Kim, and J. R. Greer *Phys. Rev. Lett.* **100**, 155502 (2008);
<http://www.jrgreer.caltech.edu/>
- ¹³ COMSOL Multiphysics Version 3.4, COMSOL AB, Tegnérgatan 23, SE-111 40, Stockholm, Sweden.
www.comsol.com.